

Parton-Hadron Duality in Unpolarised and Polarised Structure Functions

N. Bianchi* and A. Fantoni†

Laboratori Nazionali di Frascati dell'INFN, Via E. Fermi 40, 00044 Frascati (RM), Italy

S. Liuti‡

University of Virginia, Charlottesville, Virginia 22901, USA.

(Dated: October 8, 2018)

We study the phenomenon of parton-hadron duality in both polarised and unpolarised electron proton scattering using the HERMES and the Jefferson Lab data, respectively. In both cases we extend a systematic perturbative QCD based analysis to the integrals of the structure functions in the resonance region. After subtracting target mass corrections and large x resummation effects, we extract the remaining power corrections up to order $1/Q^2$. We find a sizeable suppression of these terms with respect to analyses using deep inelastic scattering data. The suppression appears consistently in both polarised and unpolarised data, except for the low Q^2 polarised data, where a large negative higher twist contribution remains. Possible scenarios generating this behavior are discussed.

PACS numbers: 13.88.+e, 13.60.Hb

I. INTRODUCTION

The structure of hadrons and their interactions can be described within two different but complementary approaches based on either partonic or hadronic degrees of freedom. The first one is expected to be valid at high energy, while the second one is applicable at low energy where the effects of confinement become large. In some specific cases where a description in terms of non-partonic degrees of freedom seems more natural, the quark-gluon description can be also successfully used. This observation is called parton-hadron duality. It was introduced for deep inelastic scattering (DIS) by Bloom and Gilman [1] who reported an equivalence between the smooth x dependence of the inclusive structure function at large Q^2 and the average over W^2 of the nucleon resonances ($x = Q^2/2M\nu$, Q^2 is the four momentum transfer squared, M is the nucleon mass, ν is the energy transfer, and $W^2 = Q^2(1/x - 1) + M^2$ is the final state invariant mass). One refers to *global* duality if the average, defined *e.g.* as the integral of the structure functions, is taken over the whole resonance region $1 \leq W^2 \leq 4 \text{ GeV}^2$. If, however, the averaging is performed over smaller W^2 ranges, extending *e.g.* over single resonances, one can analyze the onset of *local* duality.

More generally, the concept of duality is often assumed in QCD-based interpretations of most hard scattering experiments, such as DIS, e^+e^- annihilation into hadrons, and hadron-hadron collisions. Its usage appears whenever hadronic observables (mostly averaged over a given

energy range) are replaced by calculable partonic ones with little more going into the hadronic formation phase of each process – from partons to hadrons or vice versa. In a phenomenological context, duality studies are aimed at establishing to what extent a partonic description of the hard scattering process can determine the structure of the final state. In fact, as prescribed by the factorization property of QCD, we visualize hard scattering processes happening in two stages, one dominated by short times and distances and involving only parton jets, followed by hadron formation at a much larger scale. Duality is intrinsic to the factorization property. Violations of duality might signal violations of factorization in that, for instance, the probe-parton interaction might occur at larger time scales than required in order to exclude parton (re)interactions.

With the advent of both more detailed studies of soft scales and confinement [2], and higher precision measurements covering a wide range of reactions, it is now becoming possible to investigate the role of duality in QCD as a subject per se. For example, recent studies of local parton-hadron duality and its violations in semi-leptonic decays, and τ decays illustrate how the possible impact of these experiments on the extraction of the Cabibbo-Kobayashi-Maskawa (CKM) matrix elements, depends on the size of violations of local duality [3]. A practical necessity to address duality quantitatively exists also for inclusive ep scattering where most of the currently available large x data lie in the resonance region. In fact, for $x > 0.5$ and $Q^2 \gtrsim 5 \text{ GeV}^2$ – a typical starting value for perturbative evolution – $W^2 \leq 5 \text{ GeV}^2$. Therefore, the behavior of the nucleon structure functions in the resonance region needs to be addressed in detail in order to be able to discuss theoretical predictions in the limit $x \rightarrow 1$.

The first QCD-based studies of Bloom and Gilman du-

*bianchi@lnf.infn.it

†fantoni@lnf.infn.it

‡sl4y@virginia.edu

ality reinterpreted the “averaging” procedure in terms of Mellin moments of the structure function. The moments taken in the low Q^2 and in the DIS regime, respectively, were shown to be equivalent to one another within the given range and precision of the data, modulo perturbative corrections and relatively small power corrections [4]. It was conjectured that duality resulted from a cancellation of higher order terms in the twist expansion that would otherwise be expected to dominate the cross section at $x \rightarrow 1$. This view has been adopted since, particularly in the more recent studies in Ref. [5]. In Ref. [6] a new analysis was performed, using the recent inclusive unpolarised electron-nucleon scattering data on hydrogen and deuterium targets from Jefferson Lab [7]. It was shown in particular that, because of the increased precision of the data, one is now able to unravel different sources of scaling violations affecting the structure functions, namely Target Mass Corrections (TMC), Large x Resummation effects (LxR), and dynamical Higher Twists (HTs), in addition to the standard Next-to-Leading-Order (NLO) perturbative evolution. As a result, contrarily to what originally deduced in *e.g.* Ref.[7], a more pronounced role of the HT terms is obtained, pointing at the fact that duality, defined on the basis of a dominance of single parton scattering, could indeed be broken.

In contrast to the extensive study of duality for the unpolarised, *i.e.* spin averaged, photo-absorption cross section, the validity of duality has not been investigated until very recently for the spin structure function g_1 , which is proportional to the spin-*dependent* photo-absorption cross section. Evidence of duality for the spin asymmetry A_1 was reported in Ref. [8]. A phenomenological study addressing parton-duality was performed in [9] using the low Q^2 data from Ref. [10]. Studies of duality for g_1 are of particular interest because they might help understanding the transition from the large Q^2 regime described by pQCD, and the $Q^2 \rightarrow 0$ limit, where the Gerasimov-Drell-Hearn sum rule is expected to apply [11]. They may also lead to a complementary method to study the spin structure of the nucleon at large x , which is difficult to measure in the DIS region with high statistics. In particular, they might provide additional information on the transition from single parton scattering, to the dominance of processes where several partons are involved [12]. In this respect, it is important to perform an analysis aimed at disentangling the different contributions to the Q^2 dependence of g_1 in the resonance region. The aim of this paper is to carry out such an analysis by investigating quantitatively the onset of duality and its violations both for the unpolarised and polarised structure functions.

In Section II we define the concept of duality and we illustrate the role of different kinematical regions; in Section III we present our analysis and we describe our results. In particular, we compare the data with perturbative-QCD predictions and we discuss in detail the contribution of different types of corrections in both

the unpolarised and polarised case. Finally, in Section IV we draw our conclusions.

II. DEFINITIONS AND KINEMATICS

Parton-hadron duality in DIS was first observed more than three decades ago. Since then it has been necessary to give new definitions of the quantities involved which can be described within QCD-based approaches. In what follows we list all such definitions.

A. Kinematical variables

Besides the scaling variable x , other variables have been used in the literature to study duality. A number of parameterisations based on these variables have been proposed that reproduce in an effective way some of the corrections to the perturbative QCD calculations that we study in this paper. The most extensively used variables are: $x' = 1/\omega'$, where $\omega' = 1/x + M^2/Q^2$. x' was originally introduced by Bloom and Gilman in order to obtain a better agreement between DIS and the resonance region; $\xi = 2x/(1 + (1 + 4x^2M^2/Q^2)^{1/2})$ [13], originally introduced to take into account the target mass effects; $x_w = Q^2 + B/(Q^2 + W^2 - M^2 + A)$, A and B being fitted parameters, used in Refs. [14, 15]. These additional variables include a Q^2 dependence that phenomenologically absorbs some of the scaling violations that are important at low Q^2 . In Fig.1 we compare their behavior vs. x for different values of Q^2 . From the figure one can see that by calculating F_2 in ξ and x' , one effectively “rescales” the structure function to lower values of x , in a Q^2 dependent way, namely the rescaling is larger at lower Q^2 .

In this paper we present results in terms of x and Q^2 and we illustrate the contributions of scaling violations of different origin on a case by case basis.

B. Unpolarised structure function.

The inclusive DIS cross section of unpolarised electrons off an unpolarised proton is written in terms of the two structure functions F_2 and F_1 ,

$$\frac{d^2\sigma}{dx dy} = \frac{4\pi\alpha^2}{Q^2 xy} \left[\left(1 - y - \frac{(Mxy)^2}{Q^2} \right) F_2 + y^2 x F_1 \right], \quad (1)$$

where $y = \nu/E$, E being the initial electron energy. The structure functions are related by the equation:

$$F_1 = F_2(1 + \gamma^2)/(2x(1 + R)), \quad (2)$$

where $\gamma^2 = 4M^2x^2/Q^2$, and R is ratio of the longitudinal to transverse virtual photo-absorption cross sections.

In QCD, F_2 is expanded in series of inverse powers of Q^2 , obtained by ordering the matrix elements in the

DIS process by increasing twist τ , which is equal to their dimension minus spin:

$$F_2(x, Q^2) = F_2^{LT}(x, Q^2) + \frac{H(x, Q^2)}{Q^2} + \mathcal{O}(1/Q^4) \quad (3)$$

The first term is the leading twist (LT), with $\tau = 2$. The terms of order $1/Q^{\tau-2}$, $\tau \geq 4$, in Eq.(3) are the higher order terms, generally referred to as higher twists (HTs). Additional corrections to the LT part due to the finite mass of the initial nucleon – the target mass corrections (TMC) – are included directly in F_2^{LT} . For Q^2 larger than $\approx 1 \text{ GeV}^2$, TMC are taken into account through the following expansion [16]:

$$F_2^{LT(TMC)}(x, Q^2) = \frac{x^2}{\xi^2 \gamma^3} F_2^{\text{Asy}}(\xi, Q^2) + \quad (4)$$

$$6 \frac{x^3 M^2}{Q^2 \gamma^4} \int_{\xi}^1 \frac{d\xi'}{\xi'^2} F_2^{\text{Asy}}(\xi', Q^2),$$

where F_2^{Asy} is the structure function in the absence of TMC. Since TMC should in principle be applied also to the HT, we disregard terms of $\mathcal{O}(1/Q^4)$ [17]. H , then, represents the “genuine” HT correction that involves interactions between the struck parton and the spectators or, formally, multi-parton correlation functions.

Parton-hadron duality in DIS is studied by considering integrals of the structure function defined as:

$$I^{\text{res}}(Q^2) = \int_{x_{\min}}^{x_{\max}} F_2^{\text{res}}(x, Q^2) dx \quad (5)$$

where F_2^{res} is evaluated using the experimental data in the resonance region. For each Q^2 value: $x_{\min} = Q^2/(Q^2 + W_{\max}^2 - M^2)$, and $x_{\max} = Q^2/(Q^2 + W_{\min}^2 - M^2)$. W_{\min} and W_{\max} delimit the resonance region. The same expression is then calculated in the same range of x and for the same value of Q^2 , using parameterisations of F_2 that reproduce the DIS behaviour of the data at large Q^2 . These parameterisations are very well constrained in the region of interest ($x > 0.3$) although they do not correspond directly to measured data. Here in fact F_2 is dominated by the valence contribution. On the contrary, by using the same procedure at low x where the singlet and gluon distributions govern F_2 , one would find much larger uncertainties in the initial low Q^2 parameterisations because of their strong correlation with the value of α_S . We present two forms for the DIS integrals:

$$I^{LT}(Q^2) = \int_{x_{\min}}^{x_{\max}} F_2^{LT}(x, Q^2) dx, \quad (6)$$

and

$$I^{HT}(Q^2) = \int_{x_{\min}}^{x_{\max}} \left(F_2^{LT}(x, Q^2) + \frac{H(x, Q^2)}{Q^2} \right) dx. \quad (7)$$

Duality is attained strictly only if the ratio:

$$R_{\text{unpol}}^{LT} = \frac{I^{\text{res}}}{I^{LT}}, \quad (8)$$

is unity. However, one can extend this definition to the ratio:

$$R_{\text{unpol}}^{HT} = \frac{I^{\text{res}}}{I^{HT}}. \quad (9)$$

The rationale for this definition is that even when including the first few terms of the twist expansion, one is embracing a partonic description of the proton.

Perturbative QCD analyses use the Mellin moments of the structure function, which allow for a direct comparison with theoretical predictions. These are defined as:

$$M_n(Q^2) = \int_0^1 dx x^{n-2} F_2(x, Q^2), \quad (10)$$

and by

$$M_n^{TMC}(Q^2) = \int_0^1 dx \xi^{n-1} \frac{F_2(x, Q^2)}{x} p_n \left(\frac{\xi}{x} \right), \quad (11)$$

$$p_n = 1 + \frac{6(n-1)}{(n+2)(n+3)} \left(\frac{\xi}{x} - 1 \right) + \frac{n(n-1)}{(n+2)(n+3)} \left(\frac{\xi}{x} - 1 \right)^2, \quad (12)$$

which takes into account TMC [13]. However, one needs in this case experimental values of the structure function in kinematics outside the resonance region. This procedure renders the comparison between theory and experiment less straightforward. The difference between the Mellin moments (Eqs.10,12) and the integrals over the resonance region – $I_n = \int_{x_{\min}}^{x_{\max}} x^{n-2} F_2^{LT}(x, Q^2) dx$ – is shown in Fig.2. The drop of the quantities I_n with respect to M_n at larger values of Q^2 , is due to the pQCD evolution of F_2 , that moves strength to lower values of x , outside the range $[x_{\max}, x_{\min}]$. In our approach we use the integrals defined in Eqs.6,7. As it can be understood also from the trend shown in Fig.2, these effectively describe duality also as a function of the average value of x in each interval $[x_{\min}(Q^2), x_{\max}(Q^2)]$. This corresponds to: $\langle x \rangle = x(W^2 \equiv 2.5 \text{ GeV}^2)$.

It is also possible to consider a third approach, namely a point by point comparison of F_2 both in the DIS and in the resonance region. The latter can in fact be fitted to a smooth curve tracing the resonances with a very high accuracy given by the increased precision of the new Jefferson Lab measurements. They are then compared directly to DIS parameterisations F_2 at the same x and Q^2 values. This procedure [6] is much less sensitive to the elastic contribution. All of the approaches described in this Section are necessary to interpret quantitatively the Q^2 dependence of duality and of its violation.

C. Polarised structure function.

The spin-dependent part of the polarised deep inelastic cross section is given by:

$$\frac{d^2\sigma}{dx dy} = \frac{e^4}{2\pi^2 Q^2} (-H_e H_N) \quad (13)$$

$$\left[\left(1 - \frac{y}{2} - \frac{y^2}{4} \gamma^2 \right) g_1(x, Q^2) - \frac{y}{2} \gamma^2 g_2(x, Q^2) \right],$$

where H_e and H_N are the polarisations of the incident electron and of the nucleon of the target, respectively.

Because of the mixing of g_1 and g_2 , a precise determination of g_1 from a longitudinally polarised target alone is not possible. The experimentally measured cross section asymmetries are the longitudinal A_{\parallel} and the transverse A_{\perp} ones, formed from combining data with opposite beam helicity:

$$A_{\parallel} = \frac{\sigma^{\downarrow\uparrow} - \sigma^{\uparrow\uparrow}}{\sigma^{\downarrow\uparrow} + \sigma^{\uparrow\uparrow}}, \quad A_{\perp} = \frac{\sigma^{\downarrow\rightarrow} - \sigma^{\uparrow\rightarrow}}{\sigma^{\downarrow\rightarrow} + \sigma^{\uparrow\rightarrow}}. \quad (14)$$

The polarised structure functions are determined from these asymmetries:

$$g_1(x, Q^2) = \frac{F_1(x, Q^2)}{d'} \left[A_{\parallel} + \tan \theta/2 \cdot A_{\perp} \right],$$

$$g_2(x, Q^2) = \frac{y F_1(x, Q^2)}{2d'} \left[\frac{E + E' \cos \theta}{E' \sin \theta} A_{\perp} - A_{\parallel} \right] \quad (15)$$

where E' is the scattered lepton energy, θ is the scattering angle, $d' = [(1 - \epsilon)(2 - y)]/[y(1 + \epsilon R(x, Q^2))]$, with ϵ being the degree of transverse polarization of the virtual photon and defined as $\epsilon^{-1} = 1 + 2(1 + \gamma^{-2}) \tan^2(\theta/2)$.

The virtual photon-absorption asymmetries A_1 and A_2 are related to the measured asymmetries by:

$$A_{\parallel} = D(A_1 + \eta A_2)$$

$$A_{\perp} = d(A_2 - \zeta A_1), \quad (16)$$

where D is the depolarization factor $D = y(2 - y)(1 + \gamma^2 y/2)/[y^2(1 + \gamma^2)(1 - 2m_e^2/Q^2) + 2(1 - y - \gamma^2 y^2/4)(1 + R)]$, and $d = D\sqrt{2\epsilon/(1 + \epsilon)}$, $\eta = 2\gamma(1 - y)/(2 - y)$ and $\zeta = \eta(1 + \epsilon)/2\epsilon$ are kinematic factors.

From the measured asymmetries A_{\parallel} and A_{\perp} , the virtual photon asymmetries can be related to the photon absorption cross section of the nucleon for a given x and Q^2 :

$$A_1 = \frac{\sigma_{1/2} - \sigma_{3/2}}{\sigma_{1/2} + \sigma_{3/2}} = \frac{\sigma_{TT}}{\sigma_T} = \frac{g_1 - \gamma^2 g_2}{F_1}$$

$$A_2 = \frac{2\sigma_{LT}}{\sigma_{1/2} + \sigma_{3/2}} = \frac{\sigma_{LT}}{\sigma_T} = \frac{\gamma(g_1 + g_2)}{F_1}. \quad (17)$$

Here $\sigma_{1/2}$ and $\sigma_{3/2}$ are the virtual photo-absorption cross section when the projection of the angular momentum of the photon-nucleon system along the incident photon direction is 1/2 or 3/2 respectively, σ_{LT} is the interference term between the transverse and longitudinal photon-nucleon amplitudes, respectively given by $\sigma_T = (\sigma_{1/2} + \sigma_{3/2})/2$ and $\sigma_{TT} = (\sigma_{1/2} - \sigma_{3/2})/2$. If only

the longitudinal asymmetry is measured, it is necessary to make an assumption for the asymmetry A_2 .

From the measured asymmetry it is possible to evaluate the polarised structure function g_1 ; in fact neglecting the term $\gamma^2 g_2$, Eq.(17) reduces to:

$$g_1(x, Q^2) \approx A_1(x) F_1(x, Q^2). \quad (18)$$

This approximation is adequate for describing the data within their given accuracy.

As for the unpolarised case, the twist expansion reads:

$$g_1(x, Q^2) = g_1^{LT}(x, Q^2) + \frac{\tilde{H}(x, Q^2)}{Q^2} + \mathcal{O}(1/Q^4), \quad (19)$$

where, using Eqs.(2,4,18):

$$g_1^{LT}(x, Q^2) = F_2^{LT}(x, Q^2) A_1^{exp}(x) \times (1 + \gamma^2)/(2x(1 + R^{exp})), \quad (20)$$

where by the superscript ‘‘exp’’ we emphasize that we have used the experimental values for the quantities under consideration.

We study parton-hadron duality by defining the integrals:

$$\tilde{\Gamma}_1^{\text{res}} = \int_{x_{\min}}^{x_{\max}} g_1^{\text{res}}(x, Q^2) dx, \quad (21)$$

where g_1^{res} is obtained from the data in the resonance region, and

$$\tilde{\Gamma}_1^{LT} = \int_{x_{\min}}^{x_{\max}} g_1^{LT}(x, Q^2) dx \quad (22a)$$

$$\tilde{\Gamma}_1^{HT} = \int_{x_{\min}}^{x_{\max}} \left(g_1^{LT}(x, Q^2) + \frac{\tilde{H}(x, Q^2)}{Q^2} \right) dx \quad (22b)$$

The ratios are given by:

$$R_{\text{pol}}^{LT} = \frac{\tilde{\Gamma}_1^{\text{res}}}{\tilde{\Gamma}_1^{LT}} \quad , \quad R_{\text{pol}}^{HT} = \frac{\tilde{\Gamma}_1^{\text{res}}}{\tilde{\Gamma}_1^{HT}}. \quad (23)$$

As for the unpolarised case, duality is verified if either ratio is unity.

III. ANALYSIS AND INTERPRETATION OF DATA

In this Section we present a quantitative analysis of the Q^2 dependence of parton-hadron duality in both polarised and unpolarised ep scattering. We take into account all current data in the resonance region, $1 \leq W^2 \leq 4 \text{ GeV}^2$. For the unpolarised case we used data obtained at Jefferson Lab in the range $0.3 \leq Q^2 \leq 5 \text{ GeV}^2$ [7], and data from SLAC ([18] and references therein) for $Q^2 \geq 4 \text{ GeV}^2$. For the polarised case there are only few experimental data in the resonance region. One set is part of

the E143 data [10], and it corresponds to $Q^2 = 0.5$ and 1.2 GeV^2 . Another set is the one from HERMES [8, 19] in the range $1.2 \leq Q^2 \leq 12 \text{ GeV}^2$.

In the polarised case the Q^2 dependence originates from the structure function F_1 and from the ratio R . In the evaluation of the denominators of Eqs.(23), we used the SLAC global analysis [20] parameterisation for R . and, for A_1 , a power law fit to the world DIS data at $x > 0.3$: $A_1 = x^{0.7}$, as already shown in Ref. [8]. This parameterisation of A_1 is constrained to 1 at $x=1$ and it does not depend on Q^2 , as indicated by experimental data in this range [21].

A. Comparison with pQCD

The unpolarised structure function F_2 was first evaluated from dynamical parameterisations, coming from the Parton Distribution Functions (PDFs): MRST [22], CTEQ [23], GRV94 [24] and GRV98 [25]. The last two parameterisations have been evaluated at Leading Order (LO) and at Next to Leading Order (NLO). All of them are pure DIS parameterisations and they were extended to the measured x and Q^2 ranges by pQCD evolution. The Q^2 evolution of the polarised parton densities is governed by the Dokshitzer-Gribov-Lipatov-Altarelli-Parisi (DGLAP) [26] equations. The results are shown in Fig.3, in the top panel for the unpolarised data and in the bottom panel for the polarised data. The uncertainty due to the use of different LO and NLO parameterisations is represented with a band; the other band represents the experimental uncertainty, calculated as the sum in quadrature of the statistical and systematic uncertainties of the data in the resonance region.

Because the structure functions are dominated by large x kinematics, DGLAP evolution proceeds only through Non-Singlet (NS) distributions. This explains why there is very little uncertainty in the extrapolation of the initial pQCD distribution to the low values of W^2 considered and the small difference between LO and NLO evolution.

Parton-hadron duality is not fulfilled by using solely the PDFs up to NLO in both the unpolarised and polarised structure functions F_2 and g_1 . However it is possible to see a different behavior between R_{unpol} and R_{pol} . In the unpolarised case the ratio is increasing with Q^2 , but for the polarised case the situation is different: while at low Q^2 the ratio is significantly below unity and shows a strong increase with Q^2 , at higher Q^2 the ratio derived from HERMES is above unity and they appear to be independent of Q^2 within error bars.

In Figure 4 we further illustrate the origin of this behavior by plotting separately the numerator (data points) and the denominator (“theoretical” curves representing a pQCD based parameterisation), of the ratios R_{unpol} and R_{pol} , respectively. We also plot the integral of F_1 (dotted line) in order to show the effect of both A_1 and of the Q^2 -dependent factors that come into play in the definition of g_1 . All quantities are plotted vs. $x \equiv \langle x \rangle$, *i.e.* the

average value of Bjorken x for each spectrum, defined in Section II. Notice that the value of $\langle x \rangle$ increases with Q^2 . The trends in the figure suggest therefore that similarly to what observed in DIS, in the resonance region there are corrections beyond DGLAP evolution that are positive at large x , and negative at smaller x , the threshold being defined by: $x \approx 0.33 - 0.43$ and $Q^2 \approx 1 \text{ GeV}^2$. However, while these corrections are comparable in size for both the polarised and unpolarised case at large x , at low x there seems to be a much larger non-perturbative effect for the polarised data. While possible explanations have been suggested *e.g.* in [27], it is clear that more data in this region would help disentangling the Q^2 dependence and the possible size of the non-perturbative effects.

B. Comparison with Phenomenological Parameterisations

The unpolarised structure function F_2 has been evaluated from three different phenomenological fits to DIS data [15, 28, 29] and scaled to the same Q^2 values as for I^{res} and $\tilde{\Gamma}_1^{\text{res}}$ to take into account the large effect of scaling violation at large x .

The parameterisation from Ref. [15] is a modification of the PDF [24] that purports to include target mass effects through an effective change of variable, higher twist effects at high x , and a factor that enables an extension of the fit down to the photoproduction limit. The ALLM parameterisation [28] is based on a reggeon and pomeron exchanges and it was constructed for the high W^2 limit. We included it because it can be extended to very low Q^2 values. The NMC parameterisation [29] includes a fit of HT terms using world data with $W^2 > 10 \text{ GeV}^2$.

The ratios $R_{\text{unpol}}^{\text{DIS}} = I^{\text{res}}/I^{\text{DIS}}$ and $R_{\text{pol}}^{\text{DIS}} = \tilde{\Gamma}_1^{\text{res}}/\tilde{\Gamma}_1^{\text{DIS}}$, where I^{DIS} and $\tilde{\Gamma}_1^{\text{DIS}}$ are the integrals calculated with these phenomenological parameterisations, are shown in Fig.5 in the top and bottom panel, respectively, for several Q^2 -values.

In the unpolarised case the slope of the ratio is less evident compared to the previous method shown in Fig.3 and the ratio is well consistent with unity for $Q^2 > 2 \text{ GeV}^2$. In the polarised case, the ratio at higher Q^2 derived from HERMES data is consistent with unity inside the experimental errors and still independent of Q^2 . However, at low Q^2 the uncertainty on the parameterisation is bigger than what found from the PDFs.

Since these phenomenological parameterisations are obtained by fitting deep-inelastic data even in the low Q^2 region, they can implicitly include non-perturbative effects and this may explain the “observation of duality”.

C. Size of Non-perturbative Contributions

In order to understand the nature of the remaining Q^2 dependence that cannot be described by NLO pQCD evolution, we studied the effect of TMC and LxR on the ratios R_{unpol}^{HT} and R_{pol}^{HT} . The analysis was performed by using x as an integration variable, which avoids the ambiguities associated to the usage of other *ad hoc* kinematical variables. We used standard input parametrizations with initial scale $Q_o^2 = 1$ GeV². Once TMC and LxR have been subtracted from the data, and assuming the validity of the twist expansion, Eqs.(3,19) in this region, one can interpret any remaining discrepancy in terms of HTs.

We notice that although we did not consider NNLO calculations, these are not expected to alter substantially our extraction since, differently from what seen originally in the case of F_3 , these have been proven to give a relatively small contribution to F_2 [30].

The value of $\alpha_S(M_Z^2)$ that was used in our calculations corresponds to the one given for the DIS parameterisations. It has been long noticed that a correlation exists between α_S and the extracted values of the HTs (see [31] and references therein and the recent highly accurate determination in Ref. [32]). It is exactly because of this correlation that we keep its value fixed from evaluations in a region where the HTs contribution is negligible. This statement is equivalent to saying that α_S cannot be extracted reliably from large x data.

TMC have been evaluated using Eq.(4) for the unpolarised case, and Eqs.(4,20) for the polarised data. Although this procedure disregards parton off-shell effects that might be important in the resonance region (see Refs.[33, 34]), we emphasize here its power expansion character, and we set as a limiting condition for its validity, that the inequality: $x^2 M^2/Q^2 < 1$, be verified [6]. Therefore, current treatments of TMC in the resonance region are uncertain for values of $Q^2 \lesssim 1.5$ GeV².

LxR effects arise formally from terms containing powers of $\ln(1-z)$, z being the longitudinal variable in the evolution equations, that are present in the Wilson coefficient functions $C(z)$. The latter relate the parton distributions to *e.g.* the structure function F_2 , according to:

$$F_2^{NS}(x, Q^2) = \frac{\alpha_s}{2\pi} \sum_q \int_x^1 dz C_{NS}(z) q_{NS}(x/z, Q^2), \quad (24)$$

where we have considered only the non-singlet (NS) contribution to F_2 since only valence quarks distributions are relevant in our kinematics. The logarithmic terms in $C_{NS}(z)$ become very large at large x , and they need to be resummed to all orders in α_S . This can be accomplished by noticing that the correct kinematical variable that determines the phase space for the radiation of gluons at large x , is $\widetilde{W}^2 = Q^2(1-z)/z$, instead of Q^2 [35, 36]. As a result, the argument of the strong coupling constant becomes z -dependent: $\alpha_S(Q^2) \rightarrow \alpha_S(Q^2(1-z)/z)$ (see

[37] and references therein). In this procedure, however, an ambiguity is introduced, related to the need of continuing the value of α_S for low values of its argument, *i.e.* for z very close to 1 [38]. The size of this ambiguity could be of the same order of the HT corrections. Nevertheless, our evaluation is largely free from this problem because of the particular kinematical conditions in the resonance region. We are in fact studying the structure functions at *fixed* W^2 , in between $1 \leq W^2 \leq 4$ GeV². Consequently Q^2 increases with x . This softens the ambiguity in α_S , and renders our procedure reliable for the extraction of HT terms. We illustrate this situation in Fig.6 where we plot the value of α_S at $Q^2 = 10$ GeV², and we compare it with the resummed value in the resonance region, at $Q^2(1-z)/z$ for a fixed average Q^2 , and at $Q^2(x)(1-z)/z$, with $Q^2(x) = W^2 \langle x \rangle / (1 - \langle x \rangle)$, and $\langle x \rangle = 0.83$.

All of the effects described in this Section are summarized in the upper panel of Fig.7. In the figure we plot the ratio R_{unpol}^{LT} , from Eq.(8), where the numerator is obtained from the experimental data, while the denominator includes the different components of our analysis, one by one. For unpolarised scattering we find that TMC and LxR diminish considerably the space left for HT contributions. The contribution of TMC is large at the largest values of Q^2 because these correspond also to large x values. Moreover, the effect of TMC is larger than the one of LxR. We have excluded from our analysis the lowest data point at $Q^2 \approx 0.4$ GeV² because of the high uncertainty in both the pQCD calculation and the subtraction of TMC. Also, the pQCD calculations at $Q^2 \approx 1$ GeV² differ from the ones obtained by using the available set of parametrizations perhaps because the latter are extrapolated well beyond their limit of validity.

Similarly, in polarised scattering the inclusion of TMC and LxR decreases the ratio R_{pol}^{LT} (Fig.7, bottom panel). However, in this case these effects are included almost completely within the error bars. We conclude that duality is strongly violated at $Q^2 < 1.7$ GeV².

The difference between unpolarised and polarised scattering at low Q^2 can be attributed *e.g.* to unmeasured, so far, Q^2 dependent effects, both in the asymmetry, A_1 , and in g_2 . Furthermore, a full treatment of the Q^2 dependence would require both a more accurate knowledge of the ratio R in the resonance region, and a simultaneous evaluation of g_2 . The present mismatch between the unpolarised and polarised low Q^2 behavior might indicate that factorization is broken differently for the two processes, and that the universality of partonic descriptions no longer holds.

In Figures 8, 9 we address explicitly the question of the size of the HT corrections. We define them for F_2 as:

$$H(x, Q^2) = Q^2 (F_2^{\text{res}}(x, Q^2) - F_2^{\text{LT}}) \quad (25a)$$

$$C_{HT}(x) = \frac{H(x, Q^2)}{F_2^{\text{pQCD}}(x/Q^2)} \equiv Q^2 \frac{F_2^{\text{res}}(x, Q^2) - F_2^{\text{LT}}}{F_2^{\text{LT}}}. \quad (25b)$$

A similar expression is assumed for g_1 . C_{HT} is the so-called factorised form obtained by assuming that the Q^2 dependences of the LT and of the HT parts are similar and therefore they cancel out in the ratio. Although the anomalous dimensions of the HT part could in principle be different, such a discrepancy has not been found so far in accurate analyses of DIS data. The HT coefficient, C_{HT} has been evaluated for the three cases listed also in Fig.7, namely with respect to the NLO pQCD calculation, to NLO+TMC and to NLO+TMC+LxR. The values of $1 + C_{HT}/Q^2$ are plotted in Fig.8 (upper panel) as a function of the average value of x for each spectrum. One can see that the NLO+TMC+LxR analysis yields very small values for C_{HT} in the whole range of x . Furthermore, the extracted values are consistent with the ones obtained in Ref.[6] using a different method, however the present extraction method gives more accurate results. Because of the increased precision of our analysis, we are able to disentangle the different effects from both TMC and LxR.

In the polarised case (Fig.8, lower panel) the HTs are small within the given precision, for $Q^2 > 1.7 \text{ GeV}^2$, but they appear to drop dramatically below zero for lower Q^2 values. The inclusion of TMC and LxR renders these terms consistent with zero at the larger Q^2 values, but it does not modify substantially their behavior at lower Q^2 .

In Fig.9 (upper panel) we compare our results in the unpolarised case to other current extractions of the same quantity. These are: *i*) the extractions from DIS data, performed with the cut: $W^2 > 10 \text{ GeV}^2$ [39, 40, 41]; *ii*) the recent DIS evaluation by S. Alekhin [30] using a cut on $W^2 > 4 \text{ GeV}^2$, and including both TMC and NNLO; *iii*) the results obtained within a fixed W^2 framework in Ref. [6], including both TMC and LxR. We notice that results obtained in Ref. [42] in the deep inelastic region also including both TMC and LxR yield small HT coefficients, consistent with the ones found in Ref. [6]. However, while most of the suppression of the HT in the resonance region is attributed to TMC, in [42] the contribution of TMC is small and the suppression is dominated by LxR. In other words, the Q^2 behavior in the DIS and resonance regions seems to be dominated by different effects. In Fig.9 (lower panel) we compare the HT coefficients in the unpolarised and polarised case. One can notice a considerable discrepancy at $Q^2 \leq 1.7 \text{ GeV}^2$.

Our detailed extraction of both the Q^2 dependence and the HTs in the resonance region establishes a background for understanding the transition between partonic and hadronic degrees of freedom. In particular, we seem to be detecting a region where the twist expansion breaks down, and at the same time, the data seem to be still far from the $Q^2 \rightarrow 0$ limit, where theoretical predictions can be made [43]. This breakpoint is marked, for instance, by the discrepancy between polarised and unpolarised scattering at $Q^2 \lesssim 1.7 \text{ GeV}^2$. More studies addressing this region will be pursued in the future, some of which are also mentioned in [6, 44]. In particular, a breakdown

of the twist expansion can be interpreted in terms of the dominance of multi-parton configurations over single parton contributions in the scattering process. In order to confirm this picture it will be necessary to both extend the studies of the twist expansion, including the possible Q^2 dependence of the HT coefficients and terms of order $\mathcal{O}(1/Q^4)$, and to perform duality studies in semi-inclusive experiments. Finally, a number of scenarios have been studied in [27], that consider $SU(6)$ quark parton model breaking effects and that preserve duality in polarised scattering. The results of Ref.[27] are consistent only with the larger Q^2 behavior of the data, although they do not address explicitly the question of duality violations.

IV. CONCLUSIONS

In summary, we presented a study of parton-hadron duality in both unpolarised and polarised scattering. The latter was obtained by using the first experimental data for the polarised structure function of the proton $g_1^p(x)$, for Q^2 values larger than 1.7 GeV^2 . Parton-hadron duality was analysed within a QCD context. A pQCD NLO analysis including target mass corrections and large x resummation effects was extended to the integrals of both unpolarised and polarised structure functions in the resonance region. Within our context, duality is satisfied if the pQCD calculations agree with the data, modulo higher twist contributions consistent with the twist expansion. Although the latter are found to be very small for the unpolarised structure function, we do not conclude that parton-hadron duality holds straightforwardly. On the contrary, our findings seem to unveil a richer Q^2 dynamics both at $x \rightarrow 1$ and at small x . This observation is substantiated by the fact that duality holds when comparing data in the resonance region with phenomenological fits which contain some additional “non conventional” Q^2 dependence, beyond what predicted by the twist expansion. Most importantly, the coefficient of the HTs extracted using data in the resonance region only, is smaller, and therefore not consistent with the one extracted in the DIS region. Finally, while the size of the HT contributions is comparable in both polarised and unpolarised scattering at larger x and Q^2 values, at low x and Q^2 we find large negative higher twists only in the polarised case.

Acknowledgments

We are indebted to S. Alekhin for discussions and for communications on his calculations prior to publication. We thank W. Melnitchouk for discussions. S.L. thanks the Gruppo III of I.N.F.N. at the Laboratori Nazionali di Frascati where this paper was completed, for their warm hospitality, and for the many lively discussions. This

work was completed under the U.S. Department of Energy grant no. DE-FG02-01ER41200.

-
- [1] E.D. Bloom and F.J. Gilman, Phys. Rev. Lett. **25**, 1140 (1970); Phys. Rev. D **4**, 2901 (1971).
- [2] M. Gockeler *et al.*, Phys. Rev. D **53**, 2317 (1996); LHPC collaboration and TXL Collaboration, D. Dolgov *et al.*, Phys. Rev. D **66**, 034506 (2002); W. Detmold, W. Melnitchouk and A.W. Thomas, Phys. Rev. D **66**, 054501 (2002).
- [3] M. Battaglia *et al.*, arXiv:hep-ph/0304132.
- [4] A. De Rujula, H. Georgi and H.D. Politzer, Phys. Lett. B **64**, 428 (1976) and Ann. Phys. **103**, 315 (1977).
- [5] I. Niculescu, *et al.*, Phys. Rev. D **60**, 094001 (1999); S. Liuti, Nucl. Phys. Proc. Suppl. **74** (1999) 380; X. Ji, and P. Unrau, Phys. Rev. D **52**, 72 (1995); G. Ricco *et al.*, Phys. Rev. C **57**, 356 (1998).
- [6] S. Liuti, R. Ent, C.E. Keppel and I. Niculescu, Phys. Rev. Lett. **89**, 162001 (2002).
- [7] I. Niculescu *et al.*, Phys. Rev. Lett. **85**, 1186 (2000).
- [8] HERMES Collaboration, A. Airapetian *et al.*, Phys. Rev. Lett. **90**, 092002 (2003).
- [9] J. Edelmann, G. Piller, N. Kaiser and W. Weise, Nucl. Phys. A **665**, 125 (2000).
- [10] E143 Collaboration, K. Abe *et al.*, Phys. Rev. D **58**, 112003 (1998).
- [11] HERMES Collaboration, A. Airapetian *et al.*, Eur. Phys. Journal **C26**, 527 (2003).
- [12] S. J. Brodsky, arXiv:hep-ph/0006310.
- [13] O. Nachtmann, Nucl. Phys. B **63**, 237 (1973).
- [14] A. Szczurek and V. Uleshchenko, Eur. Phys. Journal **C12**, 663 (2000).
- [15] A. Bodek and U.K. Yang, arXiv:hep-ex/0203009.
- [16] H. Georgi and H. D. Politzer, Phys. Rev. D **14**, 1829 (1976).
- [17] S. I. Alekhin, S. A. Kulagin and S. Liuti, arXiv:hep-ph/0304210.
- [18] L.W. Whitlow *et al.*, Phys. Lett. B **282**, 475 (1992).
- [19] A. Fantoni, Proceedings of the XL International Winter Meeting on Nuclear Physics, Bormio (Italy) Jan 21-26 2002, edited by I. Iori and A. Moroni; A. Fantoni, Eur. Phys. Journal **A17**, 385 (2003); A. Fantoni *et al.*, talk presented at *11th International Workshop On Deep Inelastic Scattering (DIS 2003)*, 23-27 Apr 2003, St. Petersburg, Russia.
- [20] L.W. Whitlow *et al.*, Phys. Lett. B **250**, 193 (1990).
- [21] E155 Collaboration, P.L. Anthony *et al.*, Phys. Lett. B **493**, 19 (2000).
- [22] A.D. Martin, R.G. Roberts and W.J. Stirling, Eur. Phys. Journal **C14**, 133 (2000).
- [23] H.L. Lai, *et al.*, Eur. Phys. Journal **C12**, 375 (2000).
- [24] M. Gluck, E. Reya, A. Vogt, Z. Phys. C **67**, 433 (1995).
- [25] M. Gluck, E. Reya, A. Vogt, Eur. Phys. Journal **C5**, 461 (1998).
- [26] L.V. Gribov and L.N. Lipatov, Yad. Fiz. **20** (1975) 181; G. Altarelli and G. Parisi, NPB **126**, 298 (1997); Yu.L. Dokshitzer, Sov. Phys. JETP **46** (1977) 641.
- [27] F. E. Close and W. Melnitchouk, arXiv:hep-ph/0302013.
- [28] H. Abramowicz and A. Levy, arXiv:hep-ph/9712415.
- [29] NMC Collaboration, P. Amaudruz *et al.* Phys. Lett. B **364**, 107 (1995).
- [30] (a) S. I. Alekhin, Phys. Rev. D **63**, 094022 (2001); *ibid.*, arXiv:hep-ph/0211096; *ibid.*, JHEP **0302**, 015 (2003) [arXiv:hep-ph/0211294]; (b) S. I. Alekhin, arXiv:hep-ph/0212370.
- [31] M. R. Pennington, Rept. Prog. Phys. **46**, 393 (1983).
- [32] S. Alekhin, Eur. Phys. Journal **C10**, 395 (1999).
- [33] W. R. Frazer and J. F. Gunion, Phys. Rev. Lett. **45**, 1138 (1980).
- [34] I. Niculescu, C. Keppel, S. Liuti and G. Niculescu, Phys. Rev. D **60**, 094001 (1999).
- [35] S. J. Brodsky and G. P. Lepage, “*Perturbative Quantum Chromodynamics*,” SLAC-PUB-2447.
- [36] D. Amati *et al.*, Nucl. Phys. B **173**, 429 (1980).
- [37] R. G. Roberts, Eur. Phys. Journal **C10**, 697 (1999).
- [38] M. R. Pennington and G. G. Ross, Phys. Lett. B **102**, 167 (1981).
- [39] M. Virchaux and A. Milsztajn, Phys. Lett. B **274**, 221 (1992).
- [40] A. D. Martin, R. G. Roberts, W. J. Stirling and R. S. Thorne, Phys. Lett. B **443**, 301 (1998).
- [41] M. Botje, Eur. Phys. J. C **14**, 285 (2000).
- [42] S. Schaefer, A. Schafer and M. Stratmann, Phys. Lett. B **514**, 284 (2001).
- [43] X. D. Ji and J. Osborne, J. Phys. G **27**, 127 (2001).
- [44] S. Liuti, Eur. Phys. Journal **A17**, 385 (2003).

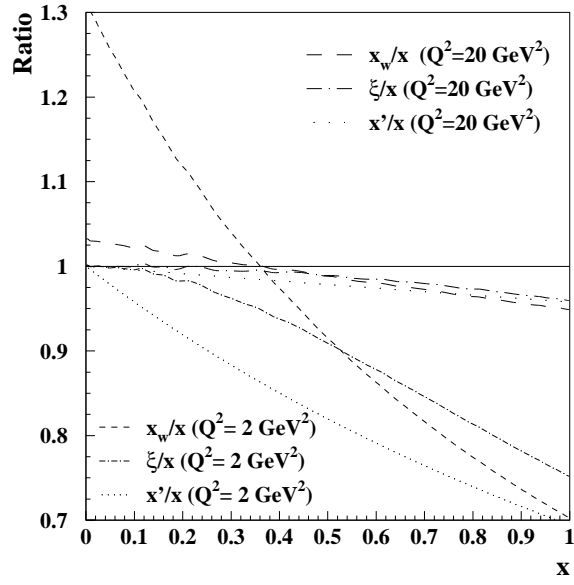


FIG. 1: Ratio between the three different variables x' , ξ and x_W defined in the text and the Bjorken variable x as a function of x .

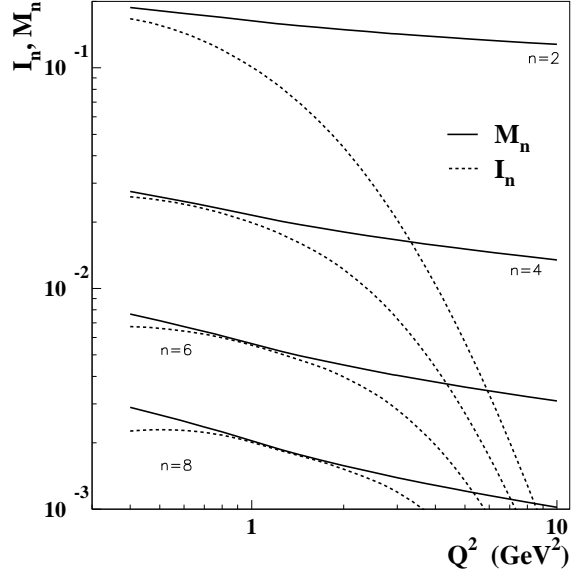


FIG. 2: The integral I_n defined in the text plotted vs. Q^2 (dashed line), compared to the Mellin moments defined in Eq.(10) (full lines). All quantities have been calculated for illustration using the parton distributions function parameterisation from Ref. [23].

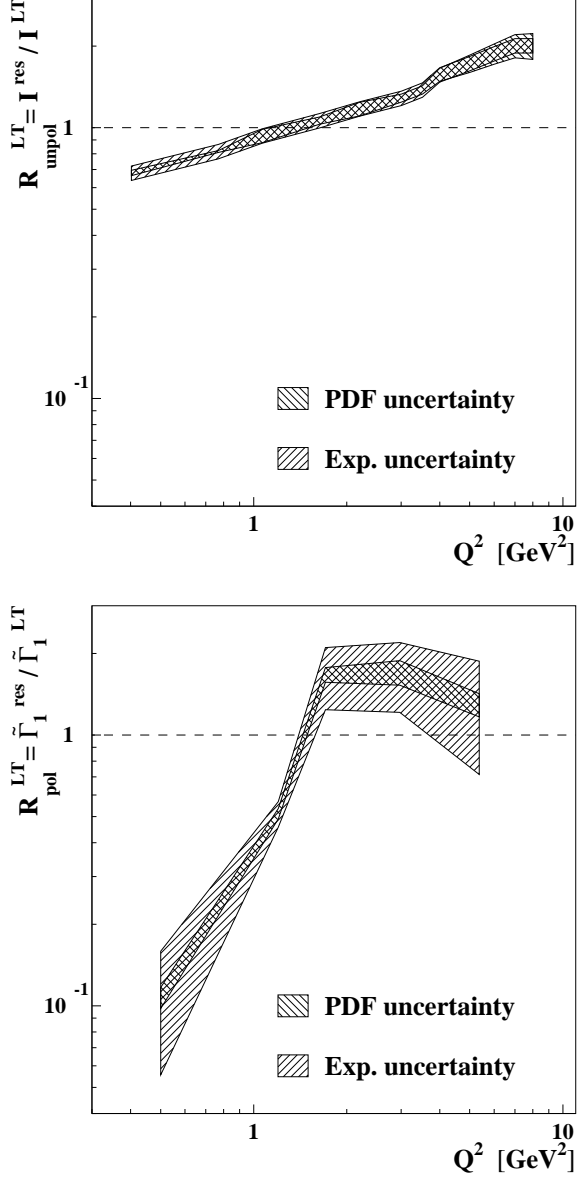


FIG. 3: Ratio between the integral of the structure function as measured in the resonance region and as parameterised in the DIS region as a function of Q^2 . The top panel refer to the unpolarised case, while the bottom panel to the polarised one. One band represents the theoretical uncertainty due to the use of different LO and NLO parameterisations: MRST [22], CTEQ [23], GRV94 [24], GRV98 [25]. The other band represents the experimental uncertainty, that is the sum in quadrature of the statistical and systematic uncertainties of the data in the resonance region.

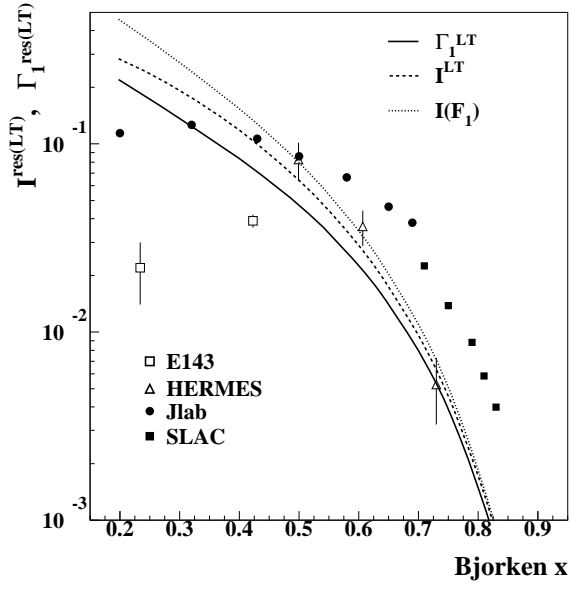


FIG. 4: The integrals I^{res} , Eq.(5), and $\tilde{\Gamma}_1^{res}$, Eq.(5) plotted vs. the average value of Bjorken x defined in the text, obtained using the data from Refs. [8, 10]. Experimental data are compared to the integrals of the valence component of the structure functions g_1 (full line), F_2 (dashed line), and F_1 (dotted line), calculated using NLO parameterisations.

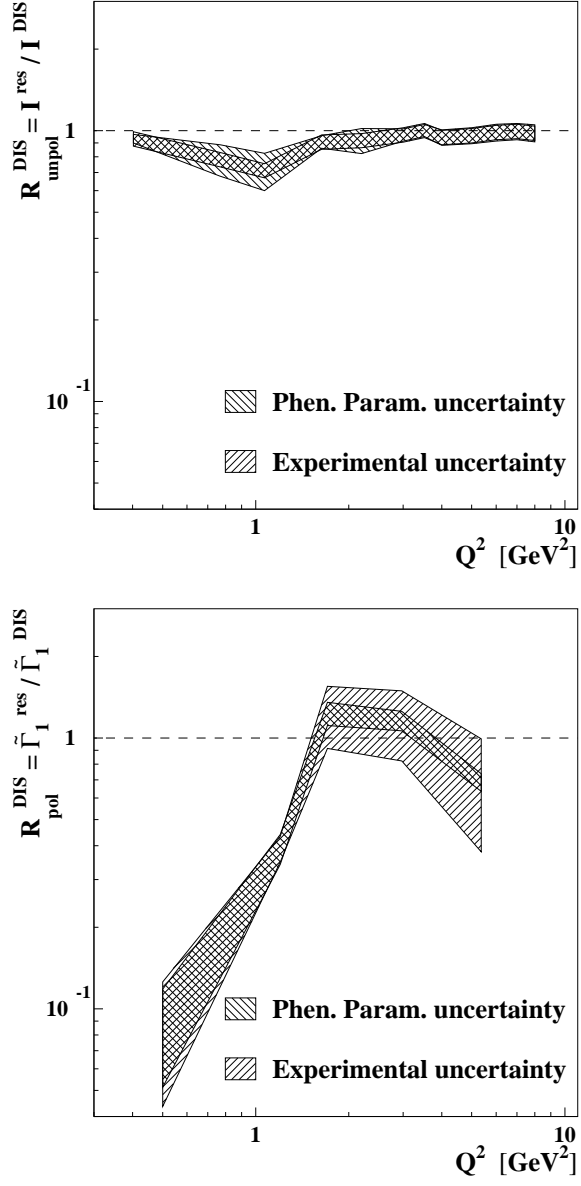


FIG. 5: Ratio between the integral of the structure function measured in the resonance region and as parameterised in the DIS region [15, 28, 29] as a function of Q^2 . The top panel refers to the unpolarised case, while the bottom panel to the polarised one. Notations are as in Fig.3.

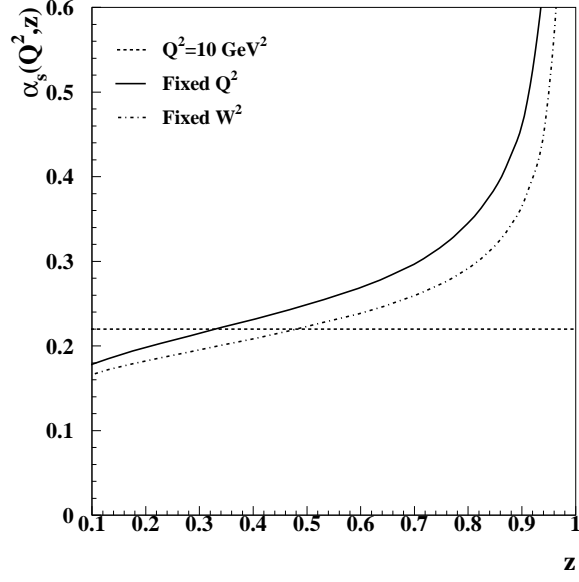


FIG. 6: α_S calculated to NLO for different forms of its argument: at $Q^2 = 10 \text{ GeV}^2$ (dashes), at $Q^2 \rightarrow Q^2(1-z)/z$ (full line), and $Q^2 \rightarrow W^2 x/(1-x)(1-z)/z$ (dot-dashed line). Calculations including LxR in the resonance region use the latter form.

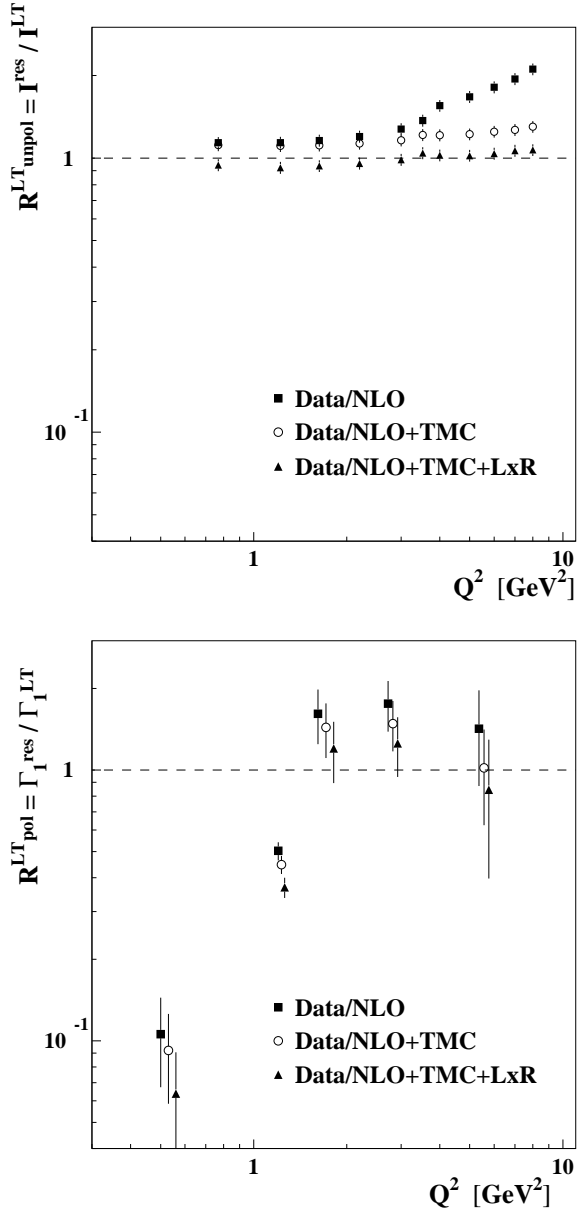


FIG. 7: Ratio between the integrals of the measured structure functions and the calculated ones plotted as a function of Q^2 . The calculation includes one by one the effects of NLO pQCD (squares), TMC (open circles) and LxR (triangles). The top panel refers to the unpolarised case, while the bottom panel refers to the polarised one.

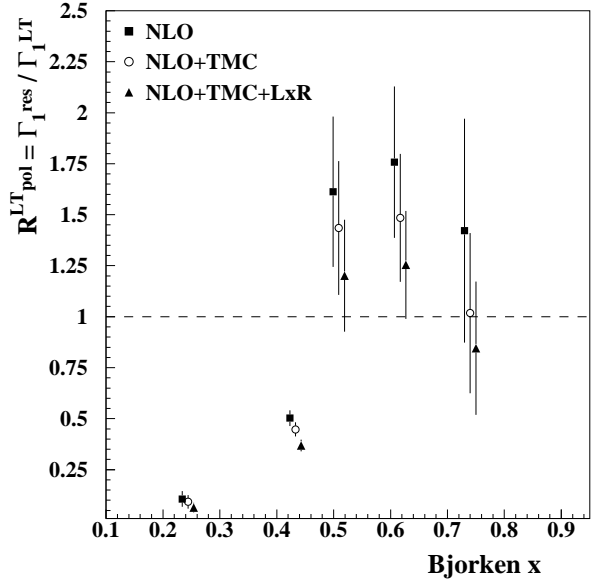
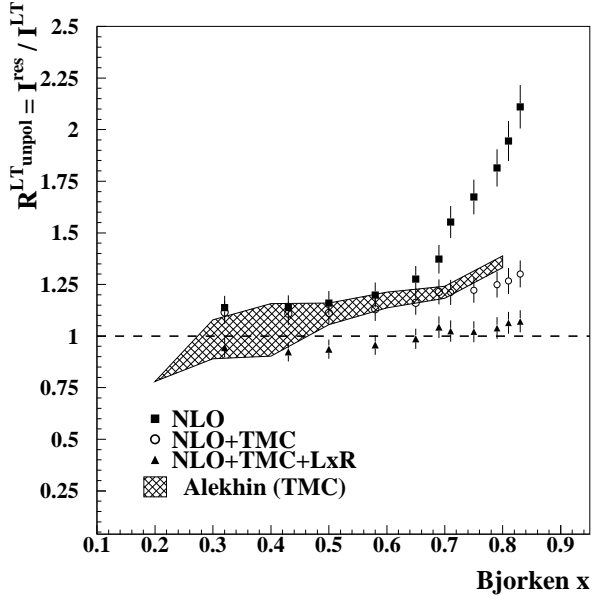


FIG. 8: HT coefficients extracted in the resonance region according to Eq.(25a). Shown in the figure is the quantity: $1 + C_{HT}(x)/Q^2$. The top panel refers to the unpolarised case, where we show the HT term obtained by considering only the NLO calculation (squares); the effect subtracting TMC (open circles); and the effects of subtracting both TMC and LxR (triangles). We show for comparison the values obtained from the coefficient H obtained in Ref.[30] using DIS data and including the effect of TMC. The bottom panel refers to the HT coefficient in the polarised case. Notations are the same as in the upper panel.

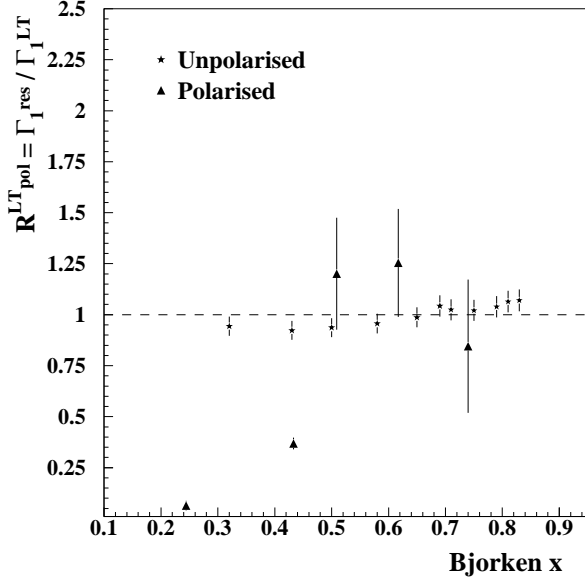
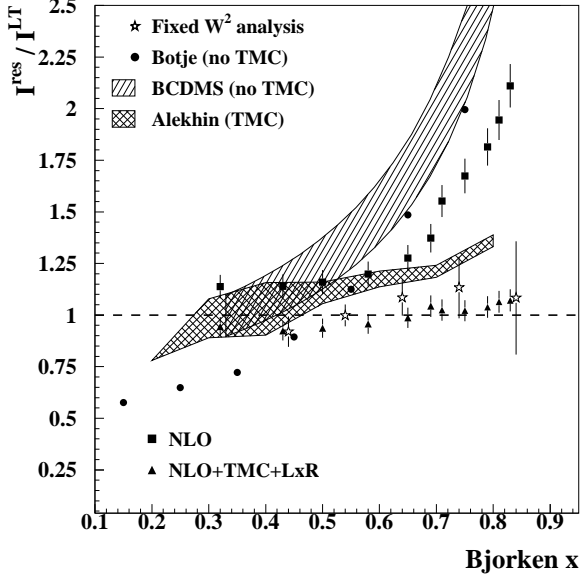


FIG. 9: Comparison of the HT coefficient displayed in Fig.8, with other extractions (upper panel). The triangles and squares are the same as in Fig.8 and they represent our determination in the resonance region. Our results are compared with extractions using DIS data only. The striped hatched area corresponds to the early extraction of Ref.[39]. The full dots are the central values of the extractions in Refs.[40] and [41]. These are compared with the more recent extraction of Ref.[30] which includes also TMC. Results obtained in the resonance region, in the fixed W^2 analysis of Ref.[6] are also shown (stars). In the bottom panel we show the comparison between the HTs in the resonance region, in the polarised (triangles) and in the unpolarised (stars) cases.